

Josephson oscillations between exciton condensates in electrostatic traps

Massimo Rontani¹ and L. J. Sham²

¹*CNR-INFM Research Center on nanoStructures and bioSystems at Surfaces (S3), Via Campi 213/A, 41125 Modena, Italy**

²*Department of Physics, University of California San Diego, La Jolla, California 92093-0319*

(Dated: July 28, 2009)

Technological advances allow for tunable lateral confinement of cold dipolar excitons in coupled quantum wells. We consider theoretically the Josephson effect between exciton condensates in two traps separated by a weak link. The flow of the exciton supercurrent is driven by the dipole energy difference between the traps. The Josephson oscillations may be observed after ensemble average of the time correlation of photons separately emitted from the two traps. The fringe visibility is controlled by the trap coupling and is robust against quantum and thermal fluctuations.

PACS numbers: 71.35.Lk, 74.50.+r, 03.75.Lm, 42.50.Ct

I. INTRODUCTION

The Josephson effect is a macroscopic coherent phenomenon which has been observed in systems as diverse as superconductors,¹ superfluid Helium,² Bose-Einstein condensates in trapped ultra-cold atomic gases.³ Since Josephson oscillations appear naturally when two spatially separated macroscopic wave functions are weakly coupled, they have been predicted for bosonic excitations in solids as well, like polaritons^{4,5} and excitons.⁶ However, unlike the polaritons, which have a photonic component allowing for easy detection,⁷ excitons stay dark unless they recombine radiatively. So far, it is unclear how the exciton Josephson effect could be observed. In this paper, we propose an experiment.

Condensed excitons are predicted to emit coherent light.⁸ If Josephson oscillations occur between two exciton traps, in principle they can be probed by measuring the interference of the beams separately emitted from the traps. However, in the time interval before recombination, there are too few photons emitted for an adequate signal to noise ratio, and one has to average the signal over many replicas of the same experiment.⁹ We will show that such ensemble averaging blurs the signature of the Josephson effect except in the relevant case of exciton “plasma” oscillations.¹⁰ For the latter the dipole energy difference between the traps modulates the visibility α of interference fringes, providing a means for detection.

The paper is organized as follows: In Sec. II we introduce the double quantum well system and illustrate a feasible scheme to manipulate electrically the exciton phase. After setting the theoretical framework (Sec. III), we discuss the proposed correlated photon counting experiment (Sec. IV) and provide an estimate for its key parameters (Sec. V).

II. ELECTRICAL CONTROL OF THE EXCITON PHASE

Consider a double quantum well where electrons and holes are separately confined in the two layers. In ex-

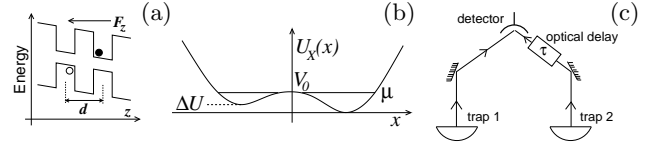


FIG. 1: (a) Double quantum well energy profile along the growth direction z . (b) Exciton potential profile of the double-trap system along x . (c) Arrangement for measuring the time correlation of the emitted photons from the two traps.

periments aiming at Bose-Einstein condensation of excitons, electron-hole pairs are optically generated off-resonance, left to thermalize, form excitons, and, at sufficiently low temperature T and high density, condense before radiative decay.¹¹ Let z be the growth axis of the two wells separated by distance d . The electrons in the conduction band and holes in the valence band move in the planes $z = d, 0$, respectively [Fig. 1(a)]. Let $\Psi_a(x, y, 0, t)$ and $\Psi_b^\dagger(x, y, d, t)$ denote the respective electron and hole destruction operators, with the vacuum being the semiconductor ground state with no excitons. In the experiments,¹¹ an electric field F_z is applied along z to suppress inter-layer tunneling, thereby quenching the exciton recombination. Fabrications¹² of electrostatic traps with suitably located electrodes to provide lateral confinement for the excitons have been implemented. The double quantum well is sandwiched between two spacer layers, providing insulation from planar electrodes lithographed on both sides of the coupled structure. Each electrode controls a tunable gate voltage, $V_g(x, y, z)$, which localizes in a region of the xy plane the field component along z , $F_z(x, y, z) = -\partial V_g(x, y, z)/\partial z$, while F_x and F_y are small and can be neglected as well as the dependence of F_z on z . The vertical field $F_z(x, y)$ makes the electrostatic potential energy of the exciton dipole depend on the lateral position, $U_X(x, y) = -edF_z(x, y)$ ($e < 0$) [cf. Fig. 1(b)]. In this way, potential traps for excitons are designed with great flexibility, with *in situ* control of the height, width, and shape of the potential barriers.¹²

First, we focus on the quasi-equilibrium situation be-

fore radiative recombination, where excitons condense in two coupled electrostatic traps, both within the condensate coherence length. Figure 1(b) depicts the exciton potential profile $U_X(x, y = 0)$ along the x axis, with a link between two identical traps. The potential barrier allows tunneling between the condensates $\Xi_1(x, y, t)$ and $\Xi_2(x, y, t)$ in the two traps.¹³ The optical coherence in a single trap is of the form

$$\Xi(x, y, t) = \langle \Psi_a^\dagger(x, y, 0, t) \Psi_b(x, y, d, t) \rangle, \quad (1)$$

where $\langle \dots \rangle$ denotes quantum and thermal average. In the limit $n a_B^2 \ll 1$, with a_B being the two-dimensional effective Bohr radius and n the exciton density, $\Xi(x, y, t)$ is the macroscopic wave function for the center-of-mass motion of excitons,¹⁴ which may be written in the form

$$\Xi(x, y, t) = \sqrt{n_s} e^{i\varphi}, \quad (2)$$

with n_s being the density of the exciton condensate and φ the phase.¹⁵ For a gauge transformation of the gate potential $V_g \rightarrow V_g - c^{-1} \partial \chi(t) / \partial t$, which leaves the field F_z unaltered, the field operators Ψ gain a phase,

$$\begin{aligned} \Psi_a &\rightarrow \Psi_a \exp \left[\frac{ie}{\hbar c} \chi(x, y, 0, t) \right], \\ \Psi_b &\rightarrow \Psi_b \exp \left[\frac{ie}{\hbar c} \chi(x, y, d, t) \right]. \end{aligned} \quad (3)$$

The macroscopic wave function, by Eq. (1), also gains a phase,

$$\varphi \rightarrow \varphi + \frac{e}{\hbar c} [\chi(z = d, t) - \chi(z = 0, t)]. \quad (4)$$

Hence, the frequency of time oscillation of the condensate is given by the electrostatic energy of the exciton dipole in the external field,¹⁶ $U = -edF_z$:

$$\varphi = \varphi^{(0)} + \frac{1}{\hbar} edF_z t, \quad (5)$$

with $\varphi^{(0)}$ being the time-independent zero-field value.¹⁷ In the absence of the bilayer separation of the electrons and the holes, their gauge phases gained in the electric field would cancel each other resulting in no time dependence driven by U . Equation (5) shows that the experimentally controllable dipole energy difference between the two traps depicted in Fig. 1(b), $\Delta U = -ed(F_{z1} - F_{z2})$, drives the relative phase between the two condensates, thereby creating Josephson oscillations as a means for measuring the Josephson tunnel between the traps.

III. EXCITON JOSEPHSON OSCILLATIONS

We next introduce the usual two-mode description of inter-trap dynamics based on the Gross-Pitaevskii (GP) equation.^{4,5,6,10,18,19} Exciton-exciton correlation²⁰ beyond the GP mean field may be neglected due to the

repulsive character of the dipolar interaction between excitons in coupled quantum wells. The condensate total wave function solution is

$$\Xi(x, y, t) = \Xi_1(x, y, N_1) e^{i\varphi_1} + \Xi_2(x, y, N_2) e^{i\varphi_2}, \quad (6)$$

where both the trap population $N_i(t)$ and the condensate phase $\varphi_i(t)$ possess the entire time dependence for the i th trap ($i = 1, 2$), and $\Xi_i(x, y, N_i)$ is a real quantity, with

$$\int dx \int dy \Xi_i^2(x, y, N_i) = N_i(t). \quad (7)$$

The dynamics of the GP macroscopic wave function $\Xi(x, y, t)$ depends entirely on the temporal evolution of two variables, the population imbalance $k(t) = (N_1 - N_2)/2$ and the relative phase $\phi(t) = \varphi_1 - \varphi_2$ of the two condensates. Here we consider a time interval much shorter than the exciton lifetime (10 — 100 ns) and ignore the spin structure. Therefore, the total population is approximately constant, $N_1(t) + N_2(t) = N$. The equations of motion for the canonically conjugated variables $\hbar k$ and ϕ are derived from the effective Hamiltonian

$$H_J = E_c \frac{k^2}{2} + \Delta U k - \frac{\delta_J}{2} \sqrt{N^2 - 4k^2} \cos \phi, \quad (8)$$

under the condition $k \ll N$ (Ref. 10). $E_c = 2d\mu_1/dN_1$ is the exciton “charging” energy of one trap, where μ_1 is the chemical potential of trap 1, whereas δ_J is the Bardeen single-particle tunnelling energy,

$$\delta_J = \frac{\hbar^2}{m} \int dy \left[\xi_1 \left(\frac{\partial \xi_2}{\partial x} \right) - \xi_2 \left(\frac{\partial \xi_1}{\partial x} \right) \right]_{x=0}, \quad (9)$$

where m is the exciton mass. The single-particle orbital $\xi_i(x, y)$ is defined through $\Xi_i(x, y) = \sqrt{N_i} \xi_i(x, y)$.

The various dynamical regimes associated to certain initial conditions ($k(0), \phi(0)$), including π oscillations and macroscopic quantum self-trapping, are exhaustively discussed in Refs. 18. Two cases are specially relevant:

1. AC Josephson effect

Under the conditions $\Delta U \gg NE_c/2$, $\Delta U \gg \delta_J$, one easily obtains

$$\phi(t) = -\frac{\Delta U}{\hbar} t + \phi(0), \quad \dot{k} = \frac{\delta_J N}{2\hbar} \sin \phi. \quad (10)$$

Equation (10) shows that, analogously to the case of two superconductors separated by a thin barrier, if the phase difference ϕ between the condensates is not a multiple of π , an exciton supercurrent $2\dot{k}$ flows across the barrier. Remarkably, in the presence of an electric field gradient along z , an exciton flux oscillates back and forth between the two traps, with frequency $\Delta U/\hbar$. As an exciton goes through the barrier, it exchanges with the field the dipole energy acquired or lost in the tunneling process. The

analogy with the AC Josephson effect for superconductors is clear: in that case a bias voltage V is applied across the junction, and the energy $2eV$ is exchanged between field and Cooper pairs, as the latter experience a potential difference of V when penetrating the potential barrier.

2. Plasma oscillations

This case concerns small oscillations around the equilibrium position $(k, \phi)_{\text{eq}} = (0, 0)$. The Hamiltonian (8) may then be linearized into the form

$$H_J = \frac{k^2}{2} \left(2 \frac{\delta_J}{N} + E_c \right) + \frac{1}{4} \delta_J N \phi^2 + \Delta U k - \frac{\delta_J N}{2}. \quad (11)$$

It follows that both k and ϕ oscillate in time with plasma frequency

$$\omega_J = \frac{1}{\hbar} \sqrt{\delta_J (N E_c / 2 + \delta_J)}. \quad (12)$$

Note that ΔU displaces the equilibrium position from $(k, \phi)_{\text{eq}} = (0, 0)$ to

$$(k, \phi)_{\text{eq}} = (-\Delta U N \delta_J / 2 (\hbar \omega_J)^2, 0). \quad (13)$$

IV. CORRELATED PHOTON COUNTING EXPERIMENT

Figure 1(c) illustrates the correlated photon counting setup which we propose to probe Josephson oscillations. The detector measures the intensity $I(\tau)$ of the sum of the two beams separately emitted from the traps. A delay time τ is induced in one of the two beams, as in Ref. 9. The fields are simply proportional to the order parameters Ξ_i of the traps. In fact, $\Xi(x, y, t)$ is associated with a macroscopic electric dipole moment, $\mathbf{P}(t) = \hat{\mathbf{x}} P_x(t) \pm i \hat{\mathbf{y}} P_y(t)$, which couples to photons: $P_x(t) = \int dx dy x \Xi(x, y, t)$, and similarly for P_y . The built-in dipole $\langle \mathbf{P}(t) \rangle \neq 0$ oscillates with frequency $(\mu + E_X)/\hbar$, where E_X is the optical gap minus the exciton binding energy, and μ accounts for exciton-exciton interaction.⁸ This macroscopic oscillating dipole is equivalent to a noiseless current, which radiates a coherent field.²¹ Therefore, the measured intensity $I(\tau)$ is $I(\tau) = 2I_0 [1 + \langle \cos \phi(\tau) \rangle]$, assuming that the fields emitted from the two traps have the same magnitude (and intensity I_0) but different relative phase ϕ , which is evaluated at the delayed time τ .²² $I(\tau)$ may be written as

$$I(\tau) = 2I_0 [1 + \alpha \cos \phi_0(\tau)], \quad (14)$$

where $\phi_0(\tau)$ is the phase averaged over many measurements, defined by the condition $\langle \sin [\phi(\tau) - \phi_0(\tau)] \rangle = 0$, and

$$\alpha = \langle \cos [\phi(\tau) - \phi_0(\tau)] \rangle \quad (15)$$

is the fringe visibility, i.e., the normalized peak-to-valley ratio of fringes, $\alpha = (I_{\text{max}} - I_{\text{min}}) / (I_{\text{max}} + I_{\text{min}})$, with I_{max} (I_{min}) being the maximum (minimum) value of $I(\tau)$, and $0 \leq \alpha \leq 1$.

Equation (14) has a few important caveats. Since $I(\tau)$ is an average, the temporal inhomogeneous effect will blur the interference fringes, i.e., $\alpha < 1$. Other dephasing mechanisms include exciton recombination and inelastic exciton-phonon scattering,⁹ as well as inelastic⁹ and elastic²³ exciton-exciton scattering, which in first instance may all be neglected for short τ , low T , and $n a_B^2 \ll 1$, respectively. The most immediate caveat is that the exciton condensates in decoupled traps must acquire a relative phase if initially they condense separately without a definite phase relation. This scenario is analogous to the case of interference between independent laser sources first discussed by Glauber²¹ and later studied experimentally for matter waves.²⁴ Even though a one-shot measurement with sufficient resolution would display fringes, the relative phase $\phi_0(\tau)$ is also subject to intrinsic dephasing effects by quantum fluctuations.²¹ The latter are significant noise sources which affect α , when ϕ and k are quantized into canonically conjugated quantum variables whereas in the GP theory used so far they were classical variables whose fluctuations were neglected.

In the following, we quantize Hamiltonian (8) in order to properly evaluate $\alpha = \langle \cos [\phi(\tau) - \phi_0(\tau)] \rangle$ as a quantum statistical average in finite traps. Therefore, we follow Ref. 25 and introduce the commutator $[\hat{\phi}, \hat{k}] = i$. The operator \hat{k} now appearing in the quantized version of Hamiltonian (8) takes the form $-i\partial/\partial\phi$, whereas the ground state wave function is defined in the space of periodic functions of ϕ with period 2π . If condensate oscillations are mainly coherent, the variance of ϕ is small and the visibility is approximated by $\alpha = 1 - \frac{1}{2} \langle (\Delta\phi)^2 \rangle$.

The most interesting case concerns plasma oscillations. For $\Delta U = 0$, the ground state of the quantized version of the harmonic oscillator Hamiltonian (11) is a Gaussian, with $\phi_0 = 0$, independent from τ , and minimal spreading $\langle \Delta\phi^2 \rangle \approx (E_c / 2\delta_J N)^{1/2}$. Therefore, the interferometer output is time-independent, $I = 2I_0(1 + \alpha)$, showing constructive interference, $I > 2I_0$, with $\alpha = 1 - (E_c / 8\delta_J N)^{1/2}$. Not surprisingly, the visibility is controlled by the ratio $E_c / \delta_J N$, reaching the maximum $\alpha = 1$ as $E_c / \delta_J N \rightarrow 0$. In fact, α is given by the balance between the competing effects of tunnelling ($\propto \delta_J N$), which enforces a well-defined inter-trap phase, and inverse compressibility ($\propto E_c$), which favors the formation of separate number states in the two traps, thus separating the two macroscopic wave functions.

A small finite value of ΔU in Eq. (11) displaces the equilibrium position of the harmonic oscillator. Noticeably, the ground state is a *coherent* state with non-null evolution of the average phase in time,

$$\phi_0(\tau) = -\frac{\Delta U}{\hbar \omega_J} \sin(\omega_J \tau), \quad (16)$$

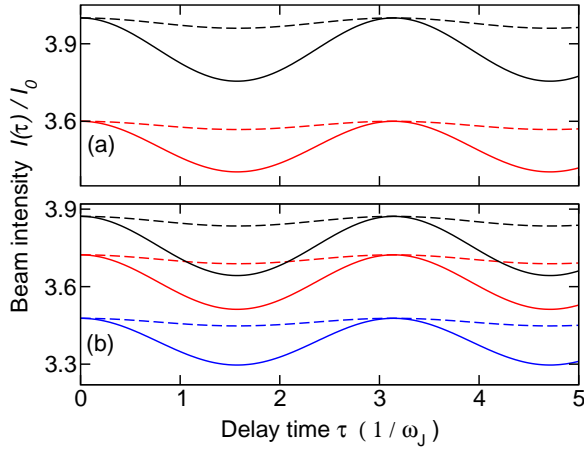


FIG. 2: (Color online). Beam intensity $I(\tau)/I_0$ vs delay time τ , for $\Delta U/\hbar\omega_J = 0.2, 0.5$ (dashed and solid lines, respectively). (a) $T = 0$ and $\alpha = 1, 0.8$ (black and red [light gray] lines, respectively). (b) $\alpha(T = 0) = 0.94$ and $k_B T/\hbar\omega_J = 0, 1, 2$ (black, red [light gray], and blue [dark gray] lines, respectively).

whereas α is unchanged. This key feature allows for directly monitoring τ -dependent plasma oscillations of frequency ω_J through the photon correlation measurement (cf. Fig. 2). We evaluate the effect of thermal fluctuations on α via the formula $\alpha(T) = \sum_n \alpha_n \exp[-\beta E_n] / \sum_n \exp[-\beta E_n]$, where $\beta = 1/k_B T$, k_B is the Boltzmann constant, $2(\alpha_n - 1) = \langle (\Delta\phi)^2 \rangle_n$ is the variance of ϕ in the n th excited state whose energy is E_n . At low T , the excited states may be approximated as those of the harmonic oscillator, giving

$$\alpha(T) = 1 - \sqrt{\frac{E_c}{2\delta_J N}} \left(\frac{1}{2} + \frac{1}{e^{\beta\hbar\omega_J} - 1} \right). \quad (17)$$

The above results are summarized by the formula

$$I(\tau) = 2I_0 \left[1 + \alpha(T) \cos\left(\frac{\Delta U}{\hbar\omega_J} \sin \omega_J \tau\right) \right], \quad (18)$$

which is valid for $E_c/\delta_J N \ll 1$. For small dipole energy variations, $\Delta U/\hbar\omega_J \ll 1$, the oscillating part within the square brackets of Eq. (18) may be written as $-\alpha(T)/2(\Delta U/\hbar\omega_J)^2 \sin^2 \omega_J \tau$. This shows that the visibility $\alpha(T)$ of fringes, which oscillate like $\sin^2 \omega_J \tau$, is modulated by the experimentally tunable factor $(\Delta U/\hbar\omega_J)^2/2$. The dependence of $I(\tau)$ on ΔU is illustrated in Fig. 2 for two values of $\Delta U/\hbar\omega_J$. As $\Delta U/\hbar\omega_J$ is increased [from 0.2 (dashed lines) to 0.5 (solid lines)], the amplitude of oscillations of $I(\tau)$ shows a strong non-linear enhancement, providing a clear signature of Josephson oscillations. The oscillation amplitudes are larger for higher values of α [cf. Fig. 2(a)], and fairly robust against thermal smearing [cf. Fig. 2(b)]. In fact, Fig. 2(b) shows that the oscillation of $I(\tau)$ is still clearly resolved for temperatures as high as $T \approx \hbar\omega_J/k_B$. At even higher temperatures $\alpha(T)$ displays anharmonic effects,²⁵ with $\alpha(T) \rightarrow 0$ as $T \rightarrow \infty$.

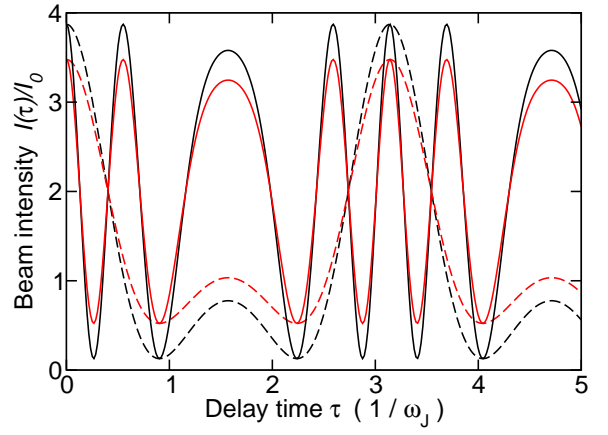


FIG. 3: (Color online). Beam intensity $I(\tau)/I_0$ vs delay time τ , for $\Delta U/\hbar\omega_J = 4, 12$ (dashed and solid lines, respectively) and $k_B T/\hbar\omega_J = 0, 2$ (black [dark gray] and red [light gray] lines, respectively), with $\alpha(T = 0) = 0.94$.

The maximum peak-to-valley ratio of fringes attainable for plasma oscillations is limited by the condition that ΔU shifts the equilibrium position $(k, \phi)_{\text{eq}}$ of the oscillator, as given in Eq. (13), slightly with respect to the origin: $\Delta U \delta_J / (\hbar\omega_J)^2 \ll 1$. For example, by taking the values of ω_J and δ_J estimated in Sec. V and imposing the condition $\Delta U \delta_J / (\hbar\omega_J)^2 = 5 \cdot 10^{-2}$, one has $\Delta U/\hbar\omega_J \approx 12$. Figure 3 displays $I(\tau)$ vs. τ for $\Delta U/\hbar\omega_J = 4, 12$ (dashed and solid lines, respectively). In both cases the range of amplitude oscillations of I is very close to the ideal interval $[0, 4I_0]$. Therefore, the intensity oscillations should be easily detected, even at finite temperatures (cf. the black [dark gray] and red [light gray] lines, corresponding to $k_B T/\hbar\omega_J = 0, 2$, respectively). For large values of $\Delta U/\hbar\omega_J$ higher overtones appear in the oscillations of $I(\tau)$ (solid lines in Fig. 3), in addition to the fundamental frequency ω_J , which is present for any finite value of ΔU (cf. dashed lines in Fig. 3).

V. ESTIMATE OF THE VISIBILITY AND PLASMA FREQUENCY

We assess the feasibility of the experiment by estimating the parameters of Eq. (18). Both α and ω_J depend on E_c and δ_J . We evaluate the latter by first solving the GP equation for a two-dimensional harmonic trap within the Thomas-Fermi approximation,¹⁰ and then by matching the wave functions of the two traps by using the semiclassical method of Ref. 19. The coupling constant $g = 4\pi d e^2 / \epsilon_r$ appearing in the non-linear term of the GP equation, multiplied by n_s , is the energy shift of an exciton added to a parallel plate capacitor with surface charge density en_s (ϵ_r is the quantum well dielectric constant).¹¹ We obtain

$$E_c = 2 \hbar\omega_0 N_1^{-1/2} \left(\frac{d}{a_B} \right)^{1/2}, \quad (19)$$

where $\hbar\omega_0$ is the energy quantum of the trap and $a_B = \hbar^2\epsilon_r/mc^2$, as well as

$$\delta_J \sim \frac{u^2}{2^{1/3}\pi} \left(\frac{a_B}{d}\right)^{2/3} \hbar\omega_0 N_1^{-2/3} e^{-S_0} [\tanh S_0/2]^{-1}. \quad (20)$$

Here $u = 0.397$, and $S_0 \sim 2^{1/2}\pi(V_0 - \mu)/\hbar\omega_0$ for a inter-trap quartic barrier of height V_0 , with $V_0 - \mu \ll V_0$ [Fig. 1(b)]. At density $n = 2.5 \cdot 10^{10} \text{ cm}^{-2}$, evaluated at the trap center, excitons are still weakly interacting ($na_B^2 \sim 0.1$ with $a_B \approx 20 \text{ nm}$). By taking GaAs parameters, $d = 12 \text{ nm}$, $N_1 = 10^3$, one has $\hbar\omega_0 = 11 \text{ } \mu\text{eV}$, $\mu_1 = 440 \text{ } \mu\text{eV}$, and a condensate radius of $1.6 \text{ } \mu\text{m}$. The barrier height V_0 , as well as S_0 , should be as low as possible. For $S_0 = 1$ we obtain high visibility [$\alpha = 0.94$ at $T = 0$, cf. Fig. 2(b)], as well as a plasma frequency $\omega_J/2\pi$ of 0.41 GHz , whose period ($\approx 2 \text{ ns}$) is an order of magnitude shorter than the exciton lifetime. Note that $\hbar\omega_J = 1.7 \text{ } \mu\text{eV} \ll \hbar\omega_0$, hence the plasma oscillation is decoupled from single-trap modes.¹⁰ The temperature associated to $\hbar\omega_J$, $T = 20 \text{ mK}$, is very low but within experimental reach.

The AC Josephson effect cannot be observed within our scheme. In fact, for large values of ΔU , the term

proportional to $\cos\phi$ appearing in the Hamiltonian (8) may be neglected in first approximation, and the ground state wave function is a plane wave, $(2\pi)^{-1/2} \exp[i\bar{n}\phi]$, where \bar{n} is the integer closest to $-\Delta U/E_c$. Since the probability density, $(2\pi)^{-1}$, is constant, the phase is distributed randomly and the visibility is zero. Therefore, the correction to α coming from the inclusion in the calculation of the term neglected in (8) will be small and fragile against fluctuations.

VI. CONCLUSION

In conclusion, exciton plasma oscillations may be measured by the time correlation of photon emission from two sides of the Josephson junction through electrical control of fringe visibility. Our findings pave the way to the observation of the exciton Josephson effect.

We acknowledge stimulating conversations with L. Butov, A. Hammack, S. Yang, I. Carusotto, V. Savona, C. Tejedor. This work is supported by CNR Short Term Mobility Program 2008 and by the NSFPIF program.

-
- * Electronic address: rontani@unimore.it;
URL: www.nanoscience.unimore.it/max.html
- ¹ A. Barone and G. Paterno, *Physics and Applications of the Josephson Effect* (Wiley, New York, 1982).
 - ² O. Avenel and E. Varoquaux, Phys. Rev. Lett. **55**, 2704 (1985); S. V. Pereverzev, A. Loshak, S. Backhaus, J. C. Davis, and R. E. Packard, Nature (London) **388**, 449 (1997); K. Sukhatme, Y. Mukharsky, T. Chui, and D. Pearson, *ibid.* **411**, 280 (2001).
 - ³ F. S. Cataliotti, S. Burger, C. Fort, P. Maddaloni, F. Minardi, A. Trombettoni, A. Smerzi, and M. Inguscio, Science **293**, 843 (2001); Y. Shin, M. Saba, T. A. Pasquini, W. Ketterle, D. E. Pritchard, and A. E. Leanhardt, Phys. Rev. Lett. **92**, 050405 (2004); M. Albiez, R. Gati, J. Fölling, S. Hunsmann, M. Cristiani, and M. K. Oberthaler, *ibid.* **95**, 010402 (2005); S. Levy, E. Lahoud, I. Shomroni, and J. Steinhauer, Nature (London) **449**, 579 (2007).
 - ⁴ M. Wouters and I. Carusotto, Phys. Rev. Lett. **99**, 140402 (2007).
 - ⁵ D. Sarchi, I. Carusotto, M. Wouters, and V. Savona, Phys. Rev. B **77**, 125324 (2008).
 - ⁶ I. A. Shelykh, D. D. Solnyshkov, G. Pavlovic, and G. Malpuech, Phys. Rev. B **78**, 041302(R) (2008).
 - ⁷ J. Keeling, F. M. Marchetti, M. H. Szymańska, and P. B. Littlewood, Semicond. Sci. Technol. **22**, R1 (2007).
 - ⁸ T. Östreich, T. Portengen, and L. J. Sham, Solid State Commun. **100**, 325 (1996); J. Fernández-Rossier, C. Tejedor, and R. Merlin, *ibid.* **108**, 473 (1998); A. Olaya-Castro, F. J. Rodríguez, L. Quiroga, and C. Tejedor, Phys. Rev. Lett. **87**, 246403 (2001).
 - ⁹ S. Yang, A. T. Hammack, M. M. Fogler, L. V. Butov, and A. C. Gossard, Phys. Rev. Lett. **97**, 187402 (2006).
 - ¹⁰ L. Pitaevskii and S. Stringari, *Bose-Einstein Condensation*

- (Oxford University Press, Oxford, 2003).
- ¹¹ L. V. Butov, J. Phys.: Condens. Matter **16**, R1577 (2004).
- ¹² A. T. Hammack, N. A. Gippius, S. Yang, G. O. Andreev, L. V. Butov, M. Hanson, and A. C. Gossard, J. Appl. Phys. **99**, 066104 (2006); A. A. High, E. E. Novitskaya, L. V. Butov, M. Hanson, and A. C. Gossard, Science **321**, 229 (2008); G. Chen, R. Rapaport, L. N. Pfeiffer, K. West, P. M. Platzman, S. Simon, Z. Vörös, and D. Snoke, Phys. Rev. B **74**, 045309 (2006).
- ¹³ Andreev-like phenomena related to coherent exciton flow have been studied in M. Rontani and L. J. Sham, Phys. Rev. Lett. **94**, 186404 (2005); Solid State Commun. **134**, 89 (2005).
- ¹⁴ L. V. Keldysh, in *Bose-Einstein Condensation*, edited by A. Griffin, D. W. Snoke, S. Stringari (Cambridge University Press, Cambridge, 1996), pp. 246-280.
- ¹⁵ Only the relative phase between the two condensates has measurable effects, see e.g. discussions in P. W. Anderson, Rev. Mod. Phys. **38**, 298 (1966); A. J. Leggett and F. Sols, Found. Phys. **21**, 353 (1991).
- ¹⁶ A. V. Balatsky, Y. N. Joglekar, and P. B. Littlewood, Phys. Rev. Lett. **93**, 266801 (2004).
- ¹⁷ Here we use the grand canonical formalism.
- ¹⁸ A. Smerzi, S. Fantoni, S. Giovanazzi, and S. R. Shenoy, Phys. Rev. Lett. **79**, 4950 (1997); S. Raghavan, A. Smerzi, S. Fantoni, and S. R. Shenoy, Phys. Rev. A **59**, 620 (1999).
- ¹⁹ I. Zapata, F. Sols, and A. J. Leggett, Phys. Rev. A **57**, R28 (1998).
- ²⁰ T. Östreich and L. J. Sham, Phys. Rev. Lett. **83**, 3510 (1999).
- ²¹ R. J. Glauber, in *Quantum Optics and Electronics*, C. DeWitt, A. Blandin, C. Cohen-Tannoudji eds. (Gordon and Breach, New York, 1965), p. 63.

- ²² Another possibility to measure the exciton Josephson effect would be the observation of Bogoliubov excitations from the spectral properties of the emitted light.⁵ A drawback of this idea is that spectral properties are not unambiguously linked to the condensed phase.
- ²³ R. Zimmermann, Phys. Stat. Sol. (b) **243**, 2358 (2006).
- ²⁴ M. R. Andrews, C. G. Townsend, H.-J. Miesner, D. S. Durfee, D. M. Kurn, and W. Ketterle, Science **275**, 637 (1997).
- ²⁵ L. Pitaevskii and S. Stringari, Phys. Rev. Lett. **87**, 180402 (2001).